TISSUE ENGINEERING: Part A
Volume 16, Number 12, 2010

DOI: 10.1089/ten.tea.2010.0234

Hydrogel Microsphere Encapsulation of a Cell-Based Gene Therapy System Increases Cell Survival of Injected Cells, Transgene Expression, and Bone Volume in a Model of Heterotopic Ossification

Ronke M. Olabisi, Ph.D.,[1] ZaWaunyka W. Lazard, B.S.,[2] Christy L. Franco, B.S.,[1] Mary A. Hall, Ph.D.,[3] Sun Kuk Kwon, Ph.D.,[3] Eva M. Sevick-Muraca, Ph.D.,[3] John A. Hipp, Ph.D.,[4] Alan R. Davis, Ph.D.,[2] Elizabeth A. Olmsted-Davis, Ph.D.,[2] and Jennifer L. West, Ph.D.[1]

Bone morphogenetic proteins (BMPs) are well known for their osteoinductive activity, yet harnessing this capacity remains a high-priority research focus. We present a novel technology that delivers high BMP-2 levels at targeted locations for rapid endochondral bone formation, enhancing our preexisting cell-based gene therapy system by microencapsulating adenovirus-transduced cells in nondegradable poly(ethylene glycol) diacrylate (PEGDA) hydrogels before intramuscular delivery. This study evaluates the *in vitro* and *in vivo* viability, gene expression, and bone formation from transgenic fibroblasts encapsulated in PEGDA microspheres. Fluorescent viability and cytotoxicity assays demonstrated >95% viability in microencapsulated cells. ELISA and alkaline phosphatase assays established that BMP-2 secretion and specific activity from microencapsulated AdBMP2-transduced fibroblasts were not statistically different from monolayer. Longitudinal transgene expression studies of AdDsRed-transduced fibroblasts, followed through live animal optical fluorescent imaging, showed that microencapsulated cells expressed longer than unencapsulated cells. When comparable numbers of microencapsulated AdBMP2-transduced cells were intramuscularly injected into mice, microcomputed tomography evaluation demonstrated that the resultant heterotopic bone formation was approximately twice the volume of unencapsulated cells. The data suggest that microencapsulation protects cells and prolongs and spatially distributes transgene expression. Thus, incorporation of PEGDA hydrogels significantly advances current gene therapy bone repair approaches.

Introduction

Although bone possesses the capacity to repair, major insults often require surgical intervention and bone grafting.[1] In the United States, ~550,000 fractures require bone grafting annually,[2] as do millions of total joint arthroplasties, spinal arthrodeses, maxillofacial surgeries, and implant fixations.[3] In an effort to circumvent the obstacles associated with grafts, researchers have used osteoinductive growth factors, such as bone morphogenetic proteins (BMPs).[4,5] BMP-2 possesses the ability to induce *de novo* bone formation at targeted locations and is FDA approved.

Nevertheless, many clinicians have found recombinant BMP-2 to have inconsistent efficacy, especially in complex clinical scenarios such as traumatic injury.[6,7] These findings have led to a renewed emphasis to develop better methods of delivering BMP-2.[8] BMPs are rapidly cleared when administered in solution,[5] necessitating a carrier, like collagen, that can retain and sequester BMPs.[4,5] BMPs have natural affinity for collagen.[2,5,8] Unfortunately, collagen can elicit an immune response,[5,9] presents handling difficulties, and does not maintain a stable form, and use of a collagen sponge reduces the bioavailability of BMP to such a degree that large amounts are necessary for a therapeutic response.[4,5,9] Given these drawbacks, the search for alternative carrier materials that are biocompatible, biodegradable, osteoinductive, and osteoconductive is of the utmost importance.[5,10]

Poly(ethylene glycol) diacrylate (PEGDA) hydrogels are widely used in tissue engineering applications because they

[1]Department of Bioengineering, Rice University, Houston, Texas.
[2]Center for Cell and Gene Therapy, Baylor College of Medicine, Houston, Texas.
[3]Center for Molecular Imaging, The University of Texas Health Science Center, Houston, Texas.
[4]Department of Orthopaedic Surgery, Baylor College of Medicine, Houston, Texas.

are bioinert and mimic many physical properties of soft tissues.[4,11] Because of the immunoprotection they can provide, hydrogels are also used for cell encapsulation.[4,11] PEGDA hydrogels have demonstrated immunoprotection of porcine islets while permitting the diffusional release of insulin, returning diabetic mice to normoglycemia.[12] Here we present the use of PEGDA hydrogels to microencapsulate cells that produce and secrete high levels of BMP-2. Previous attempts to encapsulate our cell-based gene therapy system into a macroscopic hydrogel resulted in a significant decrease in BMP-2 release and resultant bone formation as compared to unencapsulated cells.[4] Here we hypothesize that microencapsulation will permit greater BMP-2 release than macroscopic hydrogels, and that the hydrogel microspheres will protect these cells from clearance and thereby prolong their transgene expression. We first evaluate the fate of the microencapsulated cells both *in vitro* and *in vivo* through measures of viability and transgene expression. Then, we determine the microencapsulated cells efficacy in forming bone. In this study, we utilize a nonobese diabetic/severely compromised immunodeficient mouse model to evaluate our transgenic cells *in vivo* without the confounding effects of an immune system.

Materials and Methods

Cell culture

Human diploid fetal lung fibroblasts (MRC-5) were obtained from American Type Culture Collection (ATCC, Manassas, VA) and propagated in a humidified incubator at 37°C/5% CO_2 in Dulbecco's modified Eagle's medium (Sigma, St. Louis, MO) supplemented with 10% fetal bovine serum (HyClone, Logan, UT), 1000 U/L penicillin, 100 mg/L streptomycin, and 0.25 μg/mL amphotericin B (Invitrogen Life Technologies, Gaithersburg, MD).[13] Murine bone marrow stromal cells (W20-17; a gift from Genetics Institute, Cambridge, MA) were propagated as previously described.[14]

Adenoviruses and cell transduction

Replication-defective E1-E3 deleted first-generation human type 5 adenoviruses (Ad) were constructed to contain cDNAs for BMP-2, DsRed, or no transgene (Empty) in the E1 region of the virus.[15] For the viruses AdBMP2, AdDsRed, and AdEmpty, the viral particle (VP)-to-plaque-forming unit ratio was 1:83, 1:2, and 1:111, respectively, and all viruses were confirmed to be negative for replication-competent adenovirus. MRC-5 cells were transduced as previously described with AdBMP2, AdDsRed, or AdEmpty cassette at a viral concentration of 2500 VP/cell.[15,16] Briefly, virus was added to fresh supplemented Dulbecco's modified Eagle's medium and incubated with cells at 37°C overnight.

Synthesis of PEGDA

PEGDA was prepared by combining 0.4 mmol/mL acryloyl chloride, 0.2 mmol/mL triethylamine, and 0.1 mmol/mL dry PEG (10 kDa; Fluka, Milwaukee, WI) in anhydrous dichloromethane under argon overnight. The resulting PEGDA was then precipitated with ether, filtered, lyophilized, and stored under argon at −20°C. PEGDA was analyzed by proton NMR (Avance 400 MHz; Bruker, Billerica, MA; solvent, *N*,*N*-dimethylformamide-d7) and only materials with a degree of acrylation >85% were used.

Microencapsulation

Hydrogel precursor solutions were formed by combining 0.1 g/mL 10 kDa PEGDA (10% w/v) with 1.5% (v/v) triethanolamine/HEPES-buffered saline (pH 7.4), 37 mM 1-vinyl-2-pyrrolidinone, 0.1 mM eosin Y, and transduced MRC-5 cells for a final concentration of 6×10^4 cells/μL. A hydrophobic photoinitiator solution (2,2-dimethoxy-2-phenyl acetophenone in 1-vinyl-2-pyrrolidinone; 300 mg/mL) was combined in mineral oil (3 μL/mL, embryo tested, sterile filtered; Sigma-Aldrich, St. Louis, MO). The microspheres were formed after adding the hydrogel precursor solution into the mineral oil, emulsifying by vortex for 2 s while exposing to white light for an additional 20 s. Microspheres were isolated by two medium washes followed by 5 min centrifugation at 1350 rpm. Cells and microspheres were quantified by measuring the amount of soluble formazan produced by cellular reduction of the tetrazolium compound [3-(4,5-dimethylthiazol-2-yl)-5-(3-carboxymethoxyphenyl)-2-(4-sulfophenyl)-2H-tetrazolium, inner salt; MTS]. Briefly, cells were counted with a Coulter Counter and a serial dilution was used as a standard curve. Microsphere and cell samples were placed in the Transwells (0.4 μm pore polycarbonate membrane Transwell inserts; Corning, Inc., Lowell, MA) in a 24-well plate with 1 mL of culture medium, and 200 μL of CellTiter 96® AQueous One Solution Reagent was added into each well. The plate was incubated for 1 h at 37°C in a humidified, 5% CO_2 atmosphere, and then the transwells were removed and the absorbance of the medium was recorded at 490 nm. To ensure proper comparisons between the microspheres and the monolayer cells, we measured the loss of cells following the encapsulation procedure and loss in the injection needle, and then accounted for and equalized cell numbers between groups before injection.

Preparation of cells for intramuscular injection

Cells transduced with AdBMP2, AdDsRed, or AdEmpty cassette were removed with trypsin, and separated into two groups: direct injection and microencapsulation. Cells directly injected were suspended at a concentration of 5×10^6 cells per 100 μL of phosphate-buffered saline and aspirated into a syringe with a 22-gauge needle. Microencapsulated cells were encapsulated at a concentration of 5×10^6 cells per 300 μL of microspheres, which were in turn suspended in 1 mL of phosphate-buffered saline and aspirated into a syringe with an 18-gauge needle.

Viability assays

MRC-5 cells were transduced with AdBMP2, harvested, and encapsulated in microspheres as described. Microspheres were maintained in culture for 1 week post-microencapsulation, and then incubated with media and 2 μM calcein acetoxymethyl ester and 4 μM ethidium homodimer (LIVE/DEAD® Viability/Cytotoxicity Kit for mammalian cells; Invitrogen, Molecular Probes, Eugene, OR) for 20 min at 37°C in a humidified, 5% CO_2 incubator. Microspheres were imaged under a confocal microscope (ex/em ~495 nm/~515 nm). Fluorescent and differential interference

contrast projections of Z-stacks were created. The red channel was thresholded to eliminate diffuse virus staining but retain nuclear stains. Total cells were counted from differential interference contrast images, live cells from green fluorescent images, and dead cells from red fluorescent images to obtain a measure of viability.

BMP-2 quantification

BMP-2 expression was evaluated for MRC-5 cells transduced with AdBMP2 or AdEmpty4 using ELISA and alkaline phosphatase (AP) assays. ELISAs were performed with a BMP-2 Quantikine ELISA kit from R&D Systems (Minneapolis, MN) using culture supernatant collected 72 h after adenovirus transduction. Transduced cells were microencapsulated or plated directly in 0.4 μm pore polycarbonate membrane Transwell inserts (Corning, Inc.) and W20-17 cells were cultured in the wells. After 72 h, W20-17 cells were assayed for AP activity.[15] Cellular AP was extracted by conducting three freeze–thaw cycles on the W20-17 cells in a 100 $\mu M/cm^2$ concentration of 25 mM Tris-HCl (pH 8.0) and 0.5% Triton X-100. A chemiluminescent disodium 3-(4-methoxyspiroy distributes-4-yl) phenyl phosphate (CSPD) substrate with Sapphire-II enhancer (Tropix; Applied Biosystems, Foster City, CA) was added to the samples for enhanced AP sensitivity. The light output after a 2 s delay was integrated from each sample for 10 s with a luminometer (TD-20/20; Turner BioSystems, Sunnyvale, CA). AP levels were recorded in relative luminescence units. These AP levels were then normalized to protein content with the bicinchoninic acid assay. Data are presented as percent AP induction relative to that of basal control cells not exposed to BMP-2.

Animal studies

All animal studies were performed in accordance with an Institutional Animal Care and Use Committee (IACUC)–approved protocol. Microencapsulated or unencapsulated transduced cells were delivered by intramuscular injection into the hind limb quadriceps muscle of nonobese diabetic/severely compromised immunodeficient female mice (8–12 weeks old; Charles River Laboratories, Wilmington, MA) ($n = 12$).

Live animal optical fluorescence imaging

The hind limbs ($n = 12$) of six mice were imaged longitudinally for 34 days following injection of fibroblasts (±microencapsulation) transduced with AdDsRed (2500 VP/cell). Fluorescent imaging was performed at excitation and emission wavelengths of 568 nm and 610 ± 30 nm, respectively. The excitation light was supplied by a 200 mW Argon/Krypton laser (Model No. 643R-AP-A01; Melles Griot Laser Group, Carlsbad, CA), and the emission light was collected after it passed through holographic (SuperNotch-Plus™ 568 nm; Kaiser Optical Systems Inc., Ann Arbor, MI) and bandpass (HQ610/60m; Chroma Technology Corporation, Bellows Falls, VT) filters and was focused onto an electron-multiplying charge-coupled device (EMCCD) camera (Photon Max 512; Princeton Instruments, Trenton, NJ) using a Nikon camera lens (Nikkor 28 mm; Nikon, Inc., Melville, NY). Exposure times were ~200 ms. Image analysis was performed using ImageJ. Fluorescence intensity (FI) was measured and recorded for a region of interest (ROI) for each site of the animal injected with cells. The ROI dimensions were constant for every site imaged and each ROI was chosen to include the optimal fluorescent signal for the given site. A target to background ratio (TBR) of FI was calculated for each site by subtracting a background (B) ROI from the target (T) ROI, and then dividing the result by the background (B) ROI; $TBR = (T - B)/B$. The TBR value was plotted versus time (i.e., day postinjection of cells). Results represent the mean TBR of FI for unencapsulated and/or encapsulated AdDsRed or AdEmpty transduced cells ($n = 4$ per group).

Heterotopic bone assay

Microencapsulated or unencapsulated AdBMP2-transduced cells were injected into the hind limb quadriceps muscles ($n = 12$) of six mice. Animals were euthanized 2 weeks after injection of the transduced cells.

Histological analysis

Mouse hind limbs were harvested, fixed in formalin, and decalcified. Hind limbs were then divided longitudinally and sectioned from the inner surface outward. Serial sections (5 μm) encompassing the entire hind limb reactive site were prepared. Every fifth slide was stained with hematoxylin and eosin. All sections were analyzed by light microscopy.

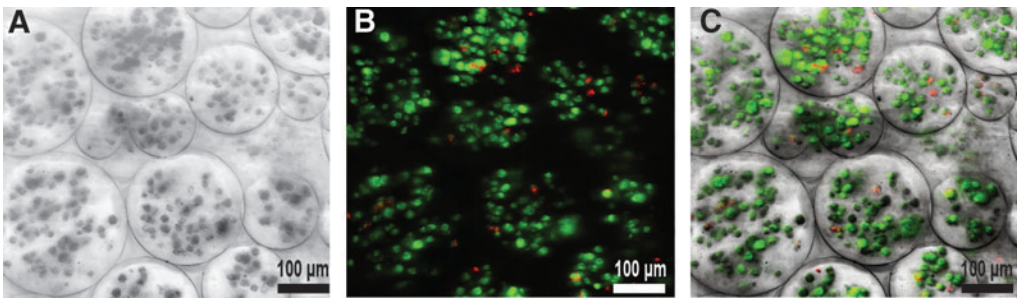

FIG. 1. Viability of AdBMP2-transduced cells (2500 VP/cell) within microspheres was assessed at day 7 using a LIVE/DEAD® Viability/Cytotoxicity Kit for mammalian cells (Invitrogen, Molecular Probes, Eugene, OR). (**A**) Minimum intensity projection of a differential interference contrast Z-stack. (**B**) Maximum intensity projection of fluorescent Z-stack merge of red and green channels. The red channel was thresholded to eliminate diffuse virus staining. Dead cells appear red and live cells appear green. (**C**) Overlay of panels (**A**) and (**B**). Living cells accounted for 95.08% ± 0.47% of total cells encapsulated. BMP, bone morphogenetic protein; VP, viral particle.

Microcomputed tomography

Microcomputed tomography (micro-CT) examinations were obtained of both legs at 15 μm resolution (eXplore Locus SP; GE Healthcare, London, ON, Canada). A hydroxyapatite phantom was scanned alongside each specimen and was used to convert the scan data from arbitrary units to units of equivalent bone density. A 3D ROI was defined for each specimen to isolate the new mineralized tissue from the normal skeletal structures (femur, tibia, and patella). The scans were thresholded to exclude any tissue with a density <100 mg/cc, and the tissue volume within the ROI was calculated as a measure of the total amount of mineralized tissue. The tissue mineral content was measured as an estimate of the total mineral in the region and the tissue density was calculated to quantify the density of the mineralized tissue. The resulting data were analyzed by one-way analysis of variance.

Statistical analysis

For BMP-2 ELISAs and AP assays, all data were taken in triplicate and reported as mean and standard deviation. Values for optical fluorescence and bone mineralization data were obtained as described and also reported as mean and standard deviation. A Student's *t*-test was performed for all measurements between controls and each experimental condition. *Post hoc* power analyses were conducted for data from *in vivo* assays to estimate the power to detect changes in gene expression and bone properties.

Results

Validation of the microspheres containing AdBMP2-transduced cells

Within the microspheres, live cells converted the nonfluorescent calcein AM into green fluorescent calcein, while ethi-

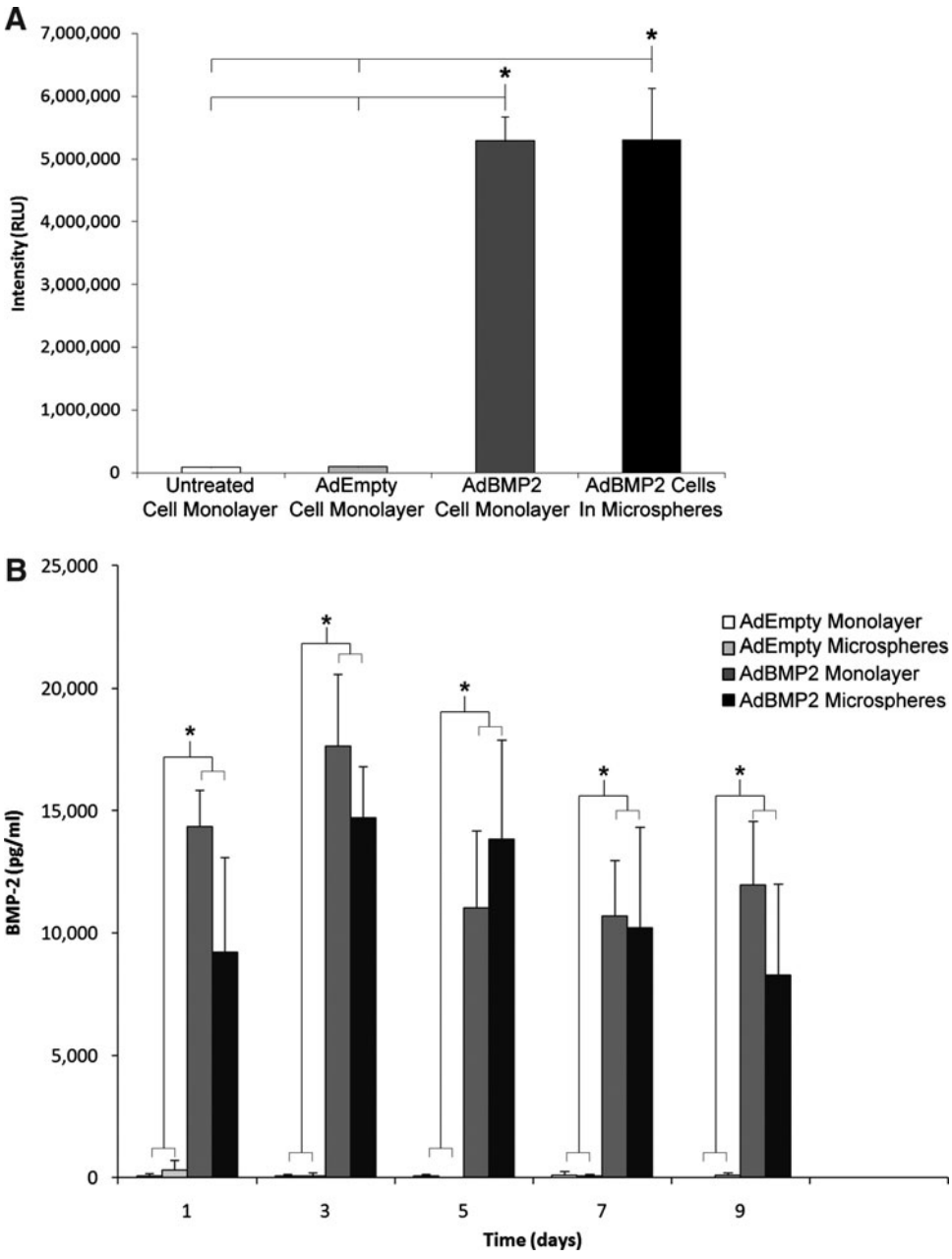

FIG. 2. Comparison of BMP-2 expression, secretion, and activity after PEGDA encapsulation. Asterisks mark significant difference ($p < 0.05$) between AdBMP2-transduced cells and controls. (**A**) BMP-2 protein in culture supernatant taken from AdBMP2- or AdEmpty cassette-transduced cells (25000 VP/cell) (monolayer), or those encapsulated in PEGDA microspheres were quantified by sampling every other day for 9 days and evaluated using an ELISA. (**B**) AP activity in W20-17 cells after addition of conditioned media from AdBMP2- or AdEmpty-transduced cells (25000 VP/cell) (monolayer), or AdBMP2-transduced cells encapsulated in PEGDA microspheres. As a negative control, we also included culture supernatant from untransduced cells. AP activity is depicted as the average RLU, where $n = 3$. Error bars represent means ± SD for $n = 3$. A Student's *t*-test was applied to demonstrate significance. AdBMP2-transduced monolayer and microsphere groups had significantly greater AP activity and BMP-2 concentration levels ($p < 0.05$) when compared against other groups, but no differences when compared to each other. In other words, microencapsulation had no effect on BMP-2 release and function. AP, alkaline phosphatase; PEGDA, poly(ethylene glycol) diacrylate; RLU, relative chemiluminescence units.

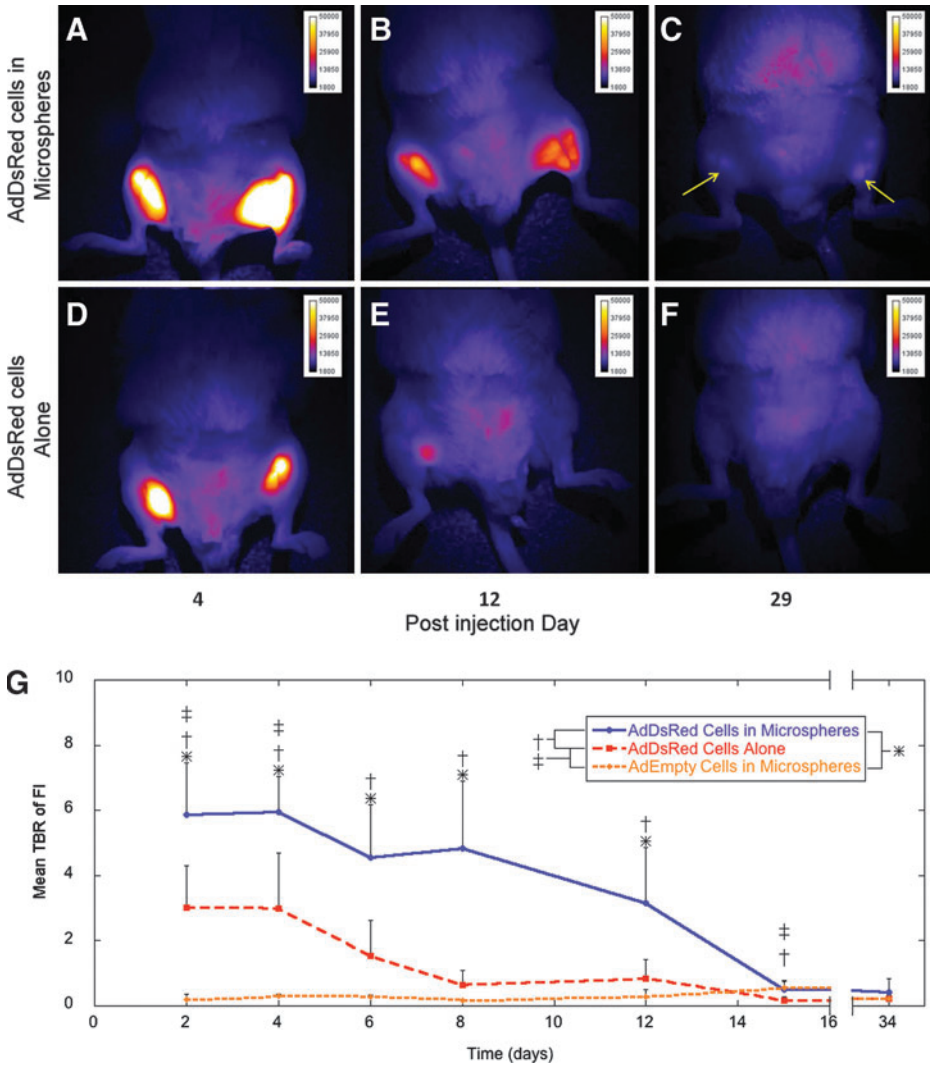

FIG. 3. Optical fluorescence imaging of mice injected with cells expressing dsRed. (**A–C**) Images of a representative mouse ($n = 4$) injected with dsRed-expressing cells encapsulated in microspheres. Arrows indicate faint fluorescent signal, (**D–F**) Images of a mouse injected with DsRed-expressing cells directly, without microspheres. The images were taken at 4, 12, and 29 days postinjection of cells. By day 29, the fluorescent signal is at background levels or undetectable for the mouse given dsRed-expressing cells without microspheres (**F**). Whereas, the signal remains detectable in the mouse given dsRed-expressing cells encapsulated in microspheres (**C**). (**G**) Mean TBR of FI in mice given unencapsulated dsRed cells, microencapsulated dsRed cells, or microencapsulated control cells. $^{*}p \leq 0.05$ for microencapsulated dsRed cells versus microencapsulated control cells; $^{\dagger}p \leq 0.05$ for microencapsulated dsRed cells versus unencapsulated dsRed cells; $^{\ddagger}p \leq 0.05$ for unencapsulated dsRed cells versus microencapsulated control cells. FI, fluorescence intensity; TBR, target-to-background ratio.

dium homodimer freely passed through the permeable membranes of dead cells to bind the DNA and fluoresce red (Fig. 1). Encapsulated cells showed high viability $95\% \pm 0.5\%$, suggesting that they were not adversely affected by the microencapsulation process. The AP activity of W20-17 cells exposed for 72 h to the culture supernatants from AdBMP2-transduced cells directly plated or encapsulated in microspheres was significantly elevated over control cells, but there was no difference between these groups, indicating that the BMP-2 released is functionally active (Fig. 2A). A 9 day time course of BMP-2 levels in culture supernatant was quantified by ELISA to be ~17,500 and 15,000 pg/mL for directly plated and microencapsulated cells, respectively (Fig. 2B). No BMP-2 was detected in either culture supernatant from AdEmpty cassette-transduced cells, or control cells.

In vivo *comparison of transgene expression with and without encapsulation in PEGDA hydrogel*

Two days after the initial injection of cells, dsRED expression was readily detected whether cells were encapsulated or not, and in no cases were cells or microspheres detected migrating from the injection site (Fig. 3A). The dsRED expression, as measured by FI at 610 ± 30 nm, was significantly elevated in microencapsulated Ad5dsRED-transduced cells compared to other groups (Fig. 3B). Microencapsulated control cells transduced with AdEmpty cassette had no fluorescent signal at 610 ± 30 nm, demonstrating that neither the cells nor the PEGDA were autofluorescing. FI in animals receiving Ad5dsRED-transduced cells directly injected was substantially reduced after 7 days and was indistinguishable from control. In microencapsulated Ad5dsRED-transduced cells, this 610 ± 30 nm dsRED fluorescent signal was significantly elevated over that of microencapsulated control cells for 15 days (Fig. 3B). After 15 days, these levels dropped; however, signal was still detectable (Fig. 3C, arrows) in some animals, suggesting that the microencapsulated cells remained viable to express the DsRed transgene. Statistical power to detect intensity over control ranged from 100% in microencapsulated cells to 99.7% in directly injected cells, and power to detect the difference between microencapsulated and unencapsulated cells was 88%.

In vivo *bone formation with and without microencapsulation in PEGDA hydrogels*

Micro-CT analysis of bone formation showed a significantly greater volume of heterotopic ossification in tissues

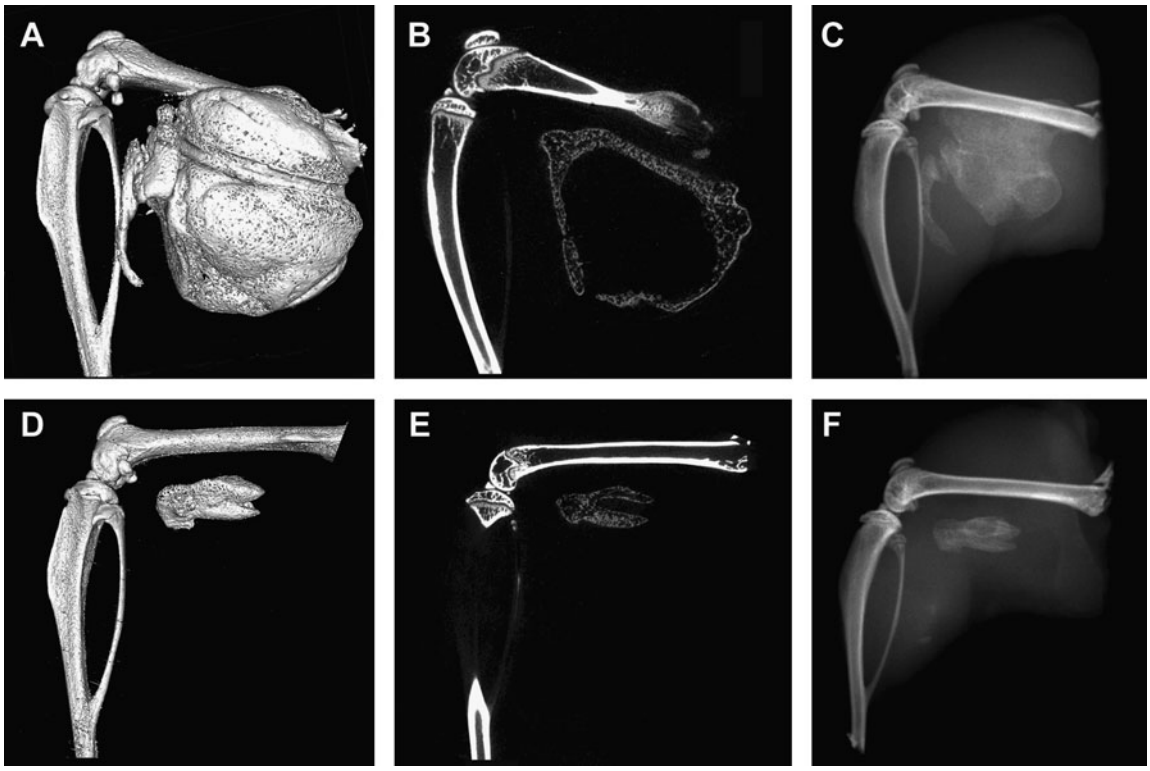

FIG. 4. Microcomputational analysis of the resultant heterotopic bone formation. (**A, D**) Three-dimensional surface renderings of the resultant heterotopic bone. (**B, E**) Cross-sectional slices through the new bone. (**C, F**) Corresponding radiograms. (**A–F**) The resultant mineralization of the muscle tissues after injection of AdBMP2-transduced cells (2500 VP/cell) encapsulated into PEGDA microspheres (**A–C**) or direct injection of unencapsulated AdBMP2-transduced cells (**D–F**). Both have a denser rim of bone, with a hollow interior structure, suggesting that the biomaterial did not alter bone patterning.

receiving microspheres (Fig. 4A–C) than those receiving directly injected cells (Fig. 4B–D). Statistical power to detect differences between volume formed in these groups was 72.5%. Cross-sectional micro-CT analysis of the newly formed bone revealed a similar architecture between the groups. Heterotopic bone formed by both the microencapsulated cells and directly injected cells had a pattern of dense bone surrounding a hollow interior (Fig. 4B,E); however, the circumference of bone within the directly injected cells was significantly smaller. Microencapsulated AdBMP2-transduced cells produced approximately twice the bone volume of unencapsulated cells (Fig. 5B). Despite the volumetric increase, the bone tissue mineral content was statistically similar between these groups, although trending toward an elevation in samples that received the microspheres (Fig. 5A). This corresponds with the change in tissue mineral density of the new bone surrounding the microspheres (Fig. 5C). The newly formed bone appears to be slightly less dense, leading to the overall similarity in mass between the two groups. Statistical power to detect differences between bone density in these groups was 76.7%.

From histological analysis, both groups had significant new bone formation within the muscle (Fig. 6). In tissues that had received the direct injection of AdBMP2-transduced cells, there was a small compact piece of bone forming a ring-like structure encircling what appears to be blood and tentative stroma, and just exterior to this structure was significant adipose (Fig. 6A). A similar structure was observed in tissues that had received microspheres (Fig. 6B). Since the microspheres did not degrade, they appear histologically as gaps or holes within the matrix (Fig. 6B). Thus, despite the presence of nondegradable microspheres, both structures were patterned to have a denser bone structure with a bone marrow-like cavity on the interior.

Discussion

Here we present a novel system for the sustained production and release of BMP-2 in a targeted manner. This approach expands on our previously reported cell-based gene therapy system, which successfully employs adenovirus transduction of fibroblasts to express high levels of BMP-2 at a targeted location.[4,13,17] High levels of BMP-2 can lead to rapid heterotopic ossification.[6,13] We previously demonstrated rapid clearance of AdBMP2-transduced cells,[13,17] thus limiting both the levels and duration of BMP-2 that can be achieved locally. Thus, we encapsulated the transduced cells within PEGDA hydrogel microspheres. Careful manipulation of their tunable physical characteristics enable PEGDA hydrogels to better approximate a tissue of interest, to regulate nutrient/waste diffusion, or to prevent interaction with immune cells.[4,11] Current carriers in clinical use, such as collagen sponges, do not retain BMP-2 efficiently, require large amounts of recombinant BMP-2 for a therapeutic effect, and are often plagued with variability,

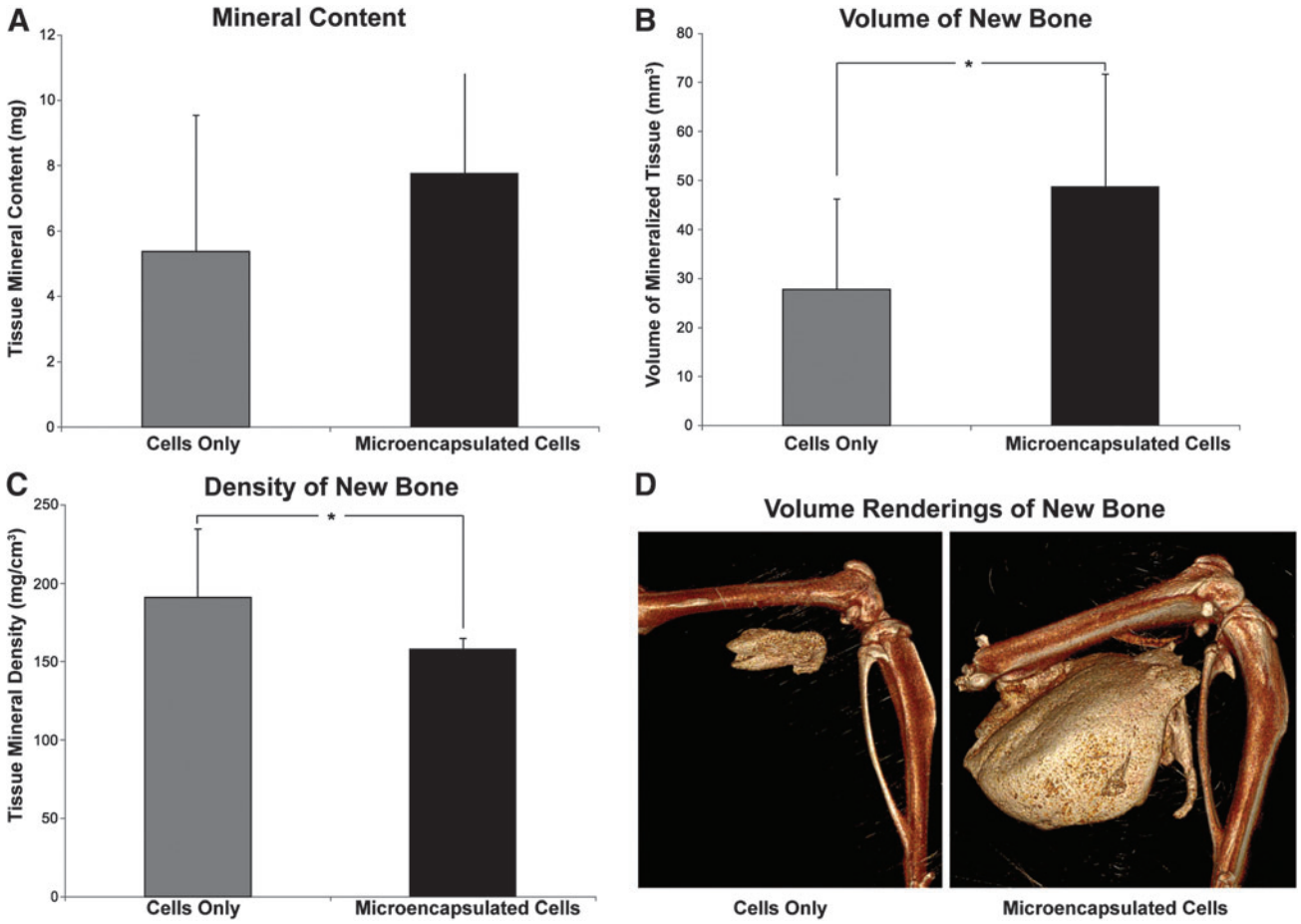

FIG. 5. Quantification of the heterotopic ossification using microcomputational analysis. Asterisks indicate statistical difference between groups ($p < 0.05$). Cells were transduced with AdBMP2 and either directly injected or encapsulated into microspheres prior to injection, and the resultant heterotopic bone was analyzed 2 weeks later. Tissue parameters: (**A**) bone tissue mineral content, (**B**) bone volume of mineralized tissue, and (**C**) bone tissue mineral density were calculated for the newly formed bone ($n = 6$ per group). The means and standard deviations for each group were calculated and compared using a one-way analysis of variance. Results indicate that mineral content is statistically equivalent ($p = 0.2$) between the groups, whereas the AdBMP2-transduced cells in microspheres had a significantly greater volume ($p = 0.038$) than the AdBMP2-transduced cells directly injected. Alternatively, the bone tissue mineral density was significantly denser for the group receiving the cells directly as compared to those in microspheres ($p = 0.029$). (**D**) A 3D volume rendering of new bone formed in cell only and microencapsulated cell groups, respectively.

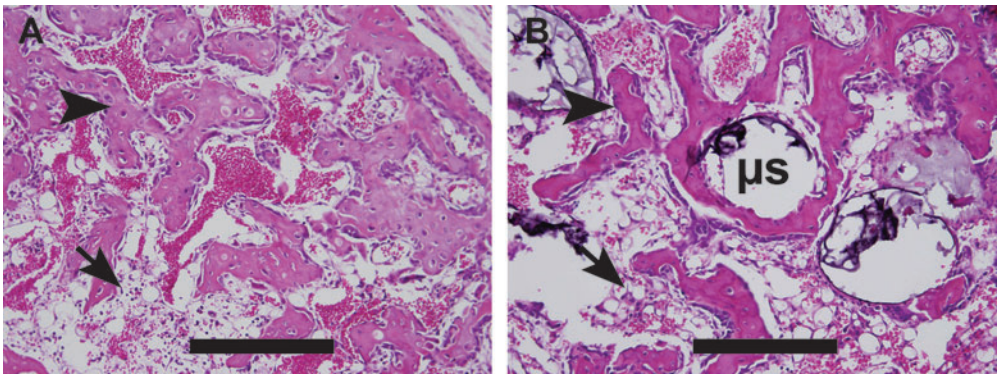

FIG. 6. Photomicrographs of heterotopic ossification. Hematoxylin and eosin stains of new bone formation by (**A**) directly injected and (**B**) microsphere (μs) encapsulated cells. Both groups show small compact pieces of bone (arrowheads) forming ring-like structures, encircling what appears to be blood and tentative stroma in the inner region, with significant adipose (arrows) just exterior to the new bone. Scale bars are 500 μm.

such as differences in handling, material properties, and, in some cases, triggering immunogenic responses.[4,5,9] Further, because collagen can bind BMP-2, our previous studies suggest that it reduced the efficacy of BMP-2 in general.[18] Additionally, the inflammation associated with the collagen sponge can also reduce the ability to produce targeted bone formation.

Our current approach avoids these issues because we use a biocompatible synthetic carrier, which minimizes immune response and does not bind BMP-2. In addition, our approach is independent of cell line, permitting the transduction of any type of cell,[19] and with efficient transduction can deliver functional BMP-2 continually to the target site over several days. Further, we are able to get high transduction efficiencies, requiring a modest quantity of cells and microspheres for a therapeutic effect. We previously implanted AdBMP2-transduced cells that were macroencapsulated in larger hydrogels to demonstrate that encapsulated cells could continue to produce bone.[4] In the current study, we demonstrate that microencapsulated cells express and release high levels of BMP-2 and produce more bone volume than unencapsulated cells. Microencapsulation permits delivery via injection, avoiding surgery.

Viability and cytotoxicity assays confirmed cell survival of the microencapsulation process, while assays to determine BMP-2 activity and release from the microspheres confirmed that the hydrogels did not impede the protein's release. The release of proteins from hydrogels is related both to diffusion distances and the hydrogel mesh size.[20] The hydrogels in the current study were formed with 10% 10 kDa PEGDA, which has been estimated to have a mesh size of 280 Å.[21] Proteins having radii smaller than the hydrogel mesh size enjoy relatively free diffusion through the polymer.[22] Mature BMP-2 is a small protein ($\sim$16 kDa), and it has been suggested that it dimerizes immediately after synthesis. The biologically active form of BMP-2 is a homodimer whose dimensions are $70\times35\times30$ Å.[23] Thus, according to the literature, our hydrogel microspheres should have released the BMP-2, which our data confirmed. ELISAs performed demonstrate equivalent BMP-2 levels from AdBMP2-transduced cells in microspheres and monolayers. The murine bone marrow stromal cell line, W20-17 cells, has been shown to respond to functional BMP-2 by undergoing osteogenesis with a rapid increase in AP.[14] AP assays using these cells showed no difference between microencapsulated and unencapsulated AdBMP2-transduced cells, demonstrating that the protein that diffused through the PEGDA hydrogel possessed similar activity as BMP-2 in culture supernatant from cells directly plated.

The millimeter-scale hydrogels employed in our previous study were a proof of concept and well exceeded the diffusion limit of oxygen.[24] The radii of the microspheres in this study were roughly in the 50–150 μm range, providing excellent cell survival. Given the same volume of PEGDA carrier, when cells were (1) encapsulated in a single hydrogel,[4] (2) equally divided into four hydrogels,[4] or (3) microencapsulated, the greatest amount of detectable BMP-2 in the culture supernatant came from the microspheres, which released identical levels as the monolayer. Our current data confirm our hypothesis that optimal BMP-2 secretion is achieved when cells are encapsulated into the smaller microsphere structures. Further, the data show that the PEGDA hydrogel material is not affecting the production, secretion, or diffusion of BMP-2 within the microspheres.

Transduction with dsRED enabled the evaluation of *in vivo* gene expression. Because solution spread is a function of injection volume,[25,26] dsRED expression in the tissues receiving the microspheres encompasses a larger volume than the unencapsulated counterpart. Although the increased volume can be explained by the difference in injection volume, the magnitude of expression should not be affected by injection volume. Nevertheless, our results demonstrate an increase in FI of microencapsulated cells for 15 days over unencapsulated cells. Since this result cannot be explained by volume difference, it suggests that the elevated intensity is a result of the microencapsulation, likely protecting these cells from clearance. This result was similar to our previous findings where the delivered cells are rapidly cleared.[13] Collectively, the data suggest that microencapsulation prolongs transgene expression within the tissues, confirming our hypothesis.

Further, *in vivo* results confirm that microencapsulation does not interfere with expression of the BMP-2 transgene. Since bone formation occurred immediately surrounding the microspheres, the volume of new bone formation corresponded to the volume of material delivered. Despite the increased volume, the mass of new bone formed was equivalent between groups. The initial bone formation response may be directly related to cell number initially injected, which was equivalent in microencapsulated and unencapsulated groups. Although previous work has demonstrated that bone is formed in as little as 1 week postinjection,[13] it is possible that our 2 week time point was too early to observe a maximal result in microspheres. The bone formation immediately adjacent to the microspheres could potentially be exploited since the microspheres can be drained and applied as a paste. Thus, exact spatial placement of the transduced cells and resultant bone formation via microsphere delivery could produce bone in a desired location of a specified shape and size. This is a critical parameter for application of the therapy to traumatic bone injury.

Surprisingly, marrow-like structures formed in both cases with similar patterning to the normal skeleton. This indicates that despite the hydrogel's capacity to dictate the shape of the newly forming bone, it does not interfere with the structural patterning that is part of the biology of bone formation.

The microspheres demonstrated their capacity to form equivalent amounts of bone to unencapsulated cells. The current study was conducted in an immune-deficient animal model to demonstrate the best bone formation results. With nonautologous cells in immune-competent animals, bone formation does not proceed. Before examining the bone-forming capacity of these cells in an immune competent animal, it was necessary to demonstrate that microsphere encapsulation did not decrease the amount of bone formed. The decreased density of the bone formed by the microspheres does not indicate poorer quality bone, but simply reflects the larger volume of bone formed: recall, density is mass/volume. When this relation is applied to our bone formation results, the calculated density corresponds well to the measured density. Moreover, the decrease in bone density is only by 17%. As aforementioned, it is possible that later time points will reveal that the microspheres' bone

density eventually reaches that of the directly injected cells. Or alternately, this 17% difference may not matter—current clinical measures of bone mineral density mark normal as ±1 standard deviation from peak bone mineral density—a measure that corresponds to bone mineral density differences of 30%.[27]

Summary and Conclusions

In this study the effect of microencapsulating AdBMP2-transduced fibroblasts before injection was evaluated. The microsphere structures were evaluated *in vitro* for viability and BMP-2 activity and secretion, and then examined *in vivo* for transgene expression and viability. Although our measures established prolonged *in vivo* expression, they did not capture a prolonged *in vivo* response, and further studies at later time points would be necessary to confirm that prolonged BMP-2 expression would lead to an increased bone formation response. Nevertheless, the hydrogel microspheres produced equivalent amounts of bone in an equivalent amount of time. This is significant because PEGDA hydrogels have demonstrated immunoprotection of xenogeneic donor cells, preserving their function.[12] This is the first step toward bone formation using nonautologous cells in an immune-competent model. Our system is the first of its kind to induce bone formation and may impact gene therapy approaches to come.

Acknowledgments

Grant support: Defense Advanced Research Projects Agency W911NF-09-1-0040 and Department of Defense W81XWH-07-0281 and W81XWH-07-1-025. The authors thank Rita Nistal for performing the histology.

Disclosure Statement

No competing financial interests exist.

References

1. Murugan, R., and Ramakrishna, S. Development of nanocomposites for bone grafting. Compos. Sci Technol **65,** 2385, 2005.
2. Mussano, F., Ciccone, G., Ceccarelli, M., Baldi, I., and Bassi, F. Bone morphogenetic proteins and bone defects: a systematic review. Spine **32,** 824, 2007.
3. Mistry, A., and Mikos, A. Tissue engineering strategies for bone regeneration. Adv Biochem Eng Biotechnol **94,** 1, 2005.
4. Bikram, M., Fouletier-Dilling, C., Hipp, J., Gannon, F., Davis, A., Olmsted-Davis, E., and West, J. Endochondral bone formation from hydrogel carriers loaded with BMP2-transduced cells. Ann Biomed Eng **35,** 796, 2007.
5. Lutolf, M., Weber, F., Schmoekel, H., Schense, J., Kohler, T., Müller, R., and Hubbell, J. Repair of bone defects using synthetic mimetics of collagenous extracellular matrices. Nat Biotechnol **21,** 513, 2003.
6. Bishop, G.B., and Einhorn, T.A. Current and future clinical applications of bone morphogenetic proteins in orthopaedic trauma surgery. Int Orthop **31,** 721, 2007.
7. Cahill, K.S., Chi, J.H., Day, A., and Claus, E.B. Prevalence, complications, and hospital charges associated with use of bone-morphogenetic proteins in spinal fusion procedures. JAMA **302,** 58, 2009.
8. Liu, Y., Hunziker, E., Vaal, C., and Groot, K. Biomimetic Coatings vs. Collagen sponges as a carrier for BMP-2: a comparison of the osteogenic responses triggered *in vivo* using an ectopic rat model. Key Eng Mater **254,** 619, 2004.
9. Schmoekel, H., Weber, F., Schense, J., Graetz, K., Schawalder, P., and Hubbell, J. Bone repair with a form of BMP-2 engineered for incorporation into fibrin cell ingrowth matrices. Biotechnol Bioeng **89,** 253, 2005.
10. Halstenberg, S., Panitch, A., Rizzi, S., Hall, H., and Hubbell, J. Biologically engineered protein-graft-poly (ethylene glycol) hydrogels: a cell adhesive and plasmin-degradable biosynthetic material for tissue repair. Biomacromolecules **3,** 710, 2002.
11. Peppas, N.A. Hydrogels. In: Ratner, B.D., Hoffman, A.S., Schoen, F.J., and Lemons, J.E., eds. Biomaterials Science: An Introduction to Materials in Medicine. San Diego: Elsevier Academic Press, 2004, pp. 100–107.
12. Cruise, G.M., Hegre, O.D., Lamberti, F.V., Hager, S.R., Hill, R., Scharp, D.S., and Hubbell, J.A. *In vitro* and *in vivo* performance of porcine islets encapsulated in interfacially photopolymerized poly (ethylene glycol) diacrylate membranes. Cell Transplant **8,** 293, 1999.
13. Fouletier-Dilling, C., Gannon, F., Olmsted-Davis, E., Lazard, Z., Heggeness, M., Shafer, J., Hipp, J., and Davis, A. Efficient and rapid osteoinduction in an immune-competent host. Hum Gene Ther **18,** 733, 2007.
14. Thies, R. Recombinant human bone morphogenetic protein-2 induces osteoblastic differentiation in W-20-17 stromal cells. Endocrinology **130,** 1318, 1992.
15. Olmsted, E., Blum, J., Rill, D., Yotnda, P., Gugala, Z., Lindsey, R., and Davis, A. Adenovirus-mediated BMP2 expression in human bone marrow stromal cells. J Cell Biochem **82,** 11, 2001.
16. Davis, A., Wivel, N., Palladino, J., Tao, L., and Wilson, J. Construction of adenoviral vectors. Mol Biotechnol **18,** 63, 2001.
17. Fouletier-Dilling, C., Bosch, P., Davis, A., Shafer, J., Stice, S., Gugala, Z., Gannon, F., and Olmsted-Davis, E. Novel compound enables high-level adenovirus transduction in the absence of an adenovirus-specific receptor. Hum Gene Ther **16,** 1287, 2005.
18. Gugala, Z., Davis, A., Fouletier-Dilling, C., Gannon, F., Lindsey, R., and Olmsted-Davis, E. Adenovirus BMP2-induced osteogenesis in combination with collagen carriers. Biomaterials **28,** 4469, 2007.
19. Gugala, Z., Olmsted-Davis, E., Gannon, F., Lindsey, R., and Davis, A. Osteoinduction by *ex vivo* adenovirus-mediated BMP2 delivery is independent of cell type. Gene Ther **10,** 1289, 2003.
20. van Dijk-Wolthuis, W.N.E., Hoogeboom, J.A.M., Van Steenbergen, M.J., Tsang, S.K.Y., and Hennink, W.E. Degradation and release behavior of dextran-based hydrogels. Macromolecules **30,** 4639, 1997.
21. Liao, H., Munoz-Pinto, D., Qu, X., Hou, Y., Grunlan, M.A., and Hahn, M.S. Influence of hydrogel mechanical properties and mesh size on vocal fold fibroblast extracellular matrix production and phenotype. Acta Biomater **4,** 1161, 2008.
22. Elbert, D.L., Pratt, A.B., Lutolf, M.P., Halstenberg, S., and Hubbell, J.A. Protein delivery from materials formed by self-selective conjugate addition reactions. J Controlled Release **76,** 11, 2001.
23. Scheufler, C., Sebald, W., and Hulsmeyer, M. Crystal structure of human bone morphogenetic protein-2 at 2.7 A resolution. J Mol Biol **287,** 103, 1999.
24. Carmeliet, P., and Jain, R.K. Angiogenesis in cancer and other diseases. Nature **407,** 249, 2000.

25. Myers, R.D. Injection of solutions into cerebral tissue: relation between volume and diffusion. Physiol Behav **1,** 171, 1966.
26. Tehovnik, E.J., and Sommer, M.A. Effective spread and timecourse of neural inactivation caused by lidocaine injection in monkey cerebral cortex. J Neurosci Methods **74,** 17, 1997.
27. Siris, E.S., Miller, P.D., Barrett-Connor, E., Faulkner, K.G., Wehren, L.E., Abbott, T.A., Berger, M.L., Santora, A.C., and Sherwood, L.M. Identification and fracture outcomes of undiagnosed low bone mineral density in postmenopausal women: results from the National Osteoporosis Risk Assessment. JAMA **286,** 2815, 2001.

Address correspondence to:
Jennifer L. West, Ph.D.
Department of Bioengineering
Rice University
6100 Main St. MS 142
Houston, TX 77005

E-mail: jwest@rice.edu

Received: April 17, 2010
Accepted: July 15, 2010
Online Publication Date: August 30, 2010